All-optical Q-switching limiter for high-power gigahertz modelocked diode-pumped solid-state lasers

Alexander Klenner* **and Ursula Keller**

Department of Physics, Institute of Quantum Electronics, ETH Zurich, 8093 Zurich, Switzerland
**klenner@phys.ethz.ch*

Abstract: Passively modelocked diode-pumped solid-state lasers (DPSSLs) with pulse repetition rates in the gigahertz regime suffer from an increased tendency for Q-switching instabilities. Low saturation fluence intracavity saturable absorbers - such as the semiconductor saturable absorber mirrors (SESAMs) - can solve this problem up to a certain average output power limited by the onset of SESAM damage. Here we present a passive stabilization mechanism, an all-optical Q-switching limiter, to reduce the impact of Q-switching instabilities and increase the potential output power of SESAM modelocked lasers in the gigahertz regime. With a proper cavity design a Kerr lens induced negative saturable absorber clamps the maximum fluence on the SESAM and therefore limits the onset of Q-switching instabilities. No critical cavity alignment is required because this Q-switching limiter acts well within the cavity stability regime. Using a proper cavity design, a high-power diode-pumped Yb:CALGO solid-state laser generated sub-100 fs pulses with an average output power of 4.1 W at a pulse repetition rate of 5 GHz. With a pulse duration of 96 fs we can achieve a peak power as high as 7.5 kW directly from the SESAM modelocked laser oscillator without any further external pulse amplification and/or pulse compression. We present a quantitative analysis of this Kerr lens induced Q-switching limiter and its impact on modelocked operation. Our work provides a route to compact high-power multi-gigahertz frequency combs based on SESAM modelocked diode-pumped solid-state lasers without any additional external amplification or pulse compression.

OCIS codes: (320.0320) Ultrafast optics; (140.0140) Lasers and laser optics; (140.3615) Lasers, ytterbium; (140.3480) Lasers, diode-pumped;

References and links

1. U. Keller, D. A. B. Miller, G. D. Boyd, T. H. Chiu, J. F. Ferguson, and M. T. Asom, "Solid-state low-loss intracavity saturable absorber for Nd:YLF lasers: an antiresonant semiconductor Fabry-Perot saturable absorber," Opt. Lett. **17**(7), 505–507 (1992).
2. U. Keller, K. J. Weingarten, F. X. Kärtner, D. Kopf, B. Braun, I. D. Jung, R. Fluck, C. Hönninger, N. Matuschek, and J. Aus der Au, "Semiconductor saturable absorber mirrors (SESAMs) for femtosecond to nanosecond pulse generation in solid-state lasers," IEEE J. Sel. Top. Quantum Electron. **2**(3), 435–453 (1996).
3. U. Keller, "Ultrafast solid-state laser oscillators: a success story for the last 20 years with no end in sight," Appl. Phys. B **100**(1), 15–28 (2010).
4. A. Schlatter, B. Rudin, S. C. Zeller, R. Paschotta, G. J. Spühler, L. Krainer, N. Haverkamp, H. R. Telle, and U. Keller, "Nearly quantum-noise-limited timing jitter from miniature Er:Yb:glass lasers," Opt. Lett. **30**(12), 1536–1538 (2005).
5. D. Hillerkuss, R. Schmogrow, T. Schellinger, M. Jordan, M. Winter, G. Huber, T. Vallaitis, R. Bonk, P. Kleinow, F. Frey, M. Roeger, S. Koenig, A. Ludwig, A. Marculescu, J. Li, M. Hoh, M. Dreschmann, J. Meyer, S. Ben Ezra, N. Narkiss, B. Nebendahl, F. Parmigiani, P. Petropoulos, B. Resan, A. Oehler, K. Weingarten, T. Ellermeyer, J. Lutz, M. Moeller, M. Huebner, J. Becker, C. Koos, W. Freude, and J. Leuthold, "26 Tbit s^{-1} line-

#233415 - $15.00 USD Received 30 Jan 2015; revised 17 Mar 2015; accepted 18 Mar 2015; published 25 Mar 2015

rate super-channel transmission utilizing all-optical fast Fourier transform processing," Nat. Photonics **5**(6), 364–371 (2011).
6. D. Hillerkuss, R. Schmogrow, M. Meyer, S. Wolf, M. Jordan, P. Kleinow, N. Lindenmann, P. C. Schindler, A. Melikyan, X. Yang, S. Ben-Ezra, B. Nebendahl, M. Dreschmann, J. Meyer, F. Parmigiani, P. Petropoulos, B. Resan, A. Oehler, K. Weingarten, L. Altenhain, T. Ellermeyer, M. Moeller, M. Huebner, J. Becker, C. Koos, W. Freude, and J. Leuthold, "Single-laser 32.4 Tbit/s Nyquist WDM transmission," J. Opt. Commun. Netw. **4**, 715–723 (2012).
7. M. Nakazawa, H. Kubota, K. Suzuki, E. Yamada, and A. Sahara, "Ultrahigh-Speed Long-Distance TDM and WDM Soliton Transmission Technologies," IEEE J. Sel. Top. Quantum Electron. **6**(2), 363–396 (2000).
8. G. A. Keeler, B. E. Nelson, D. Agarwal, C. Debaes, N. C. Helman, A. Bhatnagar, and D. A. B. Miller, "The benefits of ultrashort optical pulses in optically interconnected systems," IEEE J. Sel. Top. Quantum Electron. **9**(2), 477–485 (2003).
9. C. Debaes, A. Bhatnagar, D. Agarwal, R. Chen, G. A. Keeler, N. C. Helman, H. Thienpont, and D. A. B. Miller, "Receiver-less optical clock injection for clock distribution networks," IEEE J. Sel. Top. Quantum Electron. **9**(2), 400–409 (2003).
10. J. Boehm, "Natural user interface sensors for human body measurement," Int. Arch. Photogramm. Remote Sens. Spatial Inf. Sci. XXXIX **B3**, 531–536 (2012).
11. W. C. Swann and N. R. Newbury, "Frequency-resolved coherent lidar using a femtosecond fiber laser," Opt. Lett. **31**(6), 826–828 (2006).
12. R. Gebs, G. Klatt, C. Janke, T. Dekorsy, and A. Bartels, "High-speed asynchronous optical sampling with sub-50fs time resolution," Opt. Express **18**(6), 5974–5983 (2010).
13. P. W. Juodawlkis, J. C. Twichell, G. E. Betts, J. J. Hargreaves, R. D. Younger, J. L. Wasserman, F. J. O'Donnell, K. G. Ray, and R. C. Williamson, "Optically sampled analog-to-digital converters," IEEE Trans. Microw. Theory Tech. **49**(10), 1840–1853 (2001).
14. H. R. Telle, G. Steinmeyer, A. E. Dunlop, J. Stenger, D. H. Sutter, and U. Keller, "Carrier-envelope offset phase control: A novel concept for absolute optical frequency measurement and ultrashort pulse generation," Appl. Phys. B **69**(4), 327–332 (1999).
15. S. A. Diddams, D. J. Jones, J. Ye, S. T. Cundiff, J. L. Hall, J. K. Ranka, R. S. Windeler, R. Holzwarth, T. Udem, and T. W. Hänsch, "Direct link between microwave and optical frequencies with a 300 THz femtosecond laser comb," Phys. Rev. Lett. **84**(22), 5102–5105 (2000).
16. T. Steinmetz, T. Wilken, C. Araujo-Hauck, R. Holzwarth, T. W. Hänsch, L. Pasquini, A. Manescau, S. D'Odorico, M. T. Murphy, T. Kentischer, W. Schmidt, and T. Udem, "Laser frequency combs for astronomical observations," Science **321**(5894), 1335–1337 (2008).
17. A. Martinez and S. Yamashita, "Multi-gigahertz repetition rate passively modelocked fiber lasers using carbon nanotubes," Opt. Express **19**(7), 6155–6163 (2011).
18. S. Yamashita, Y. Inoue, K. Hsu, T. Kotake, H. Yaguchi, D. Tanaka, M. Jablonski, and S. Y. Set, "5-GHz pulsed fiber Fabry–Perot laser mode-locked using carbon nanotubes," IEEE Photon. Technol. Lett. **17**(4), 750–752 (2005).
19. A. Bartels, D. Heinecke, and S. A. Diddams, "10-GHz self-referenced optical frequency comb," Science **326**(5953), 681 (2009).
20. A. Bartels, R. Gebs, M. S. Kirchner, and S. A. Diddams, "Spectrally resolved optical frequency comb from a self-referenced 5 GHz femtosecond laser," Opt. Lett. **32**(17), 2553–2555 (2007).
21. D. E. Spence, P. N. Kean, and W. Sibbett, "60-fsec pulse generation from a self-mode-locked Ti:sapphire laser," Opt. Lett. **16**(1), 42–44 (1991).
22. M. Endo, A. Ozawa, and Y. Kobayashi, "Kerr-lens mode-locked Yb:KYW laser at 4.6-GHz repetition rate," Opt. Express **20**(11), 12191–12197 (2012).
23. M. Endo, A. Ozawa, and Y. Kobayashi, "6-GHz, Kerr-lens mode-locked Yb:Lu2O3 ceramic laser for comb-resolved broadband spectroscopy," Opt. Lett. **38**(21), 4502–4505 (2013).
24. S. Pekarek, A. Klenner, T. Südmeyer, C. Fiebig, K. Paschke, G. Erbert, and U. Keller, "Femtosecond diode-pumped solid-state laser with a repetition rate of 4.8 GHz," Opt. Express **20**(4), 4248–4253 (2012).
25. A. Diebold, F. Emaury, C. J. Saraceno, C. Schriber, M. Golling, T. Suedmeyer, and U. Keller, "SESAM mode-locked Yb:$CaGdAlO_4$ thin disk laser with 62 fs pulse generation," Opt. Lett. **38**, 3842–3845 (2013).
26. Y. Zaouter, J. Didierjean, F. Balembois, G. L. Leclin, F. Druon, P. Georges, J. Petit, P. Goldner, and B. Viana, "47-fs diode-pumped Yb^{3+}:$CaGdAlO_4$ laser," Opt. Lett. **31**(1), 119–121 (2006).
27. J. Boudeile, F. Druon, M. Hanna, P. Georges, Y. Zaouter, E. Cormier, J. Petit, P. Goldner, and B. Viana, "Continuous-wave and femtosecond laser operation of Yb:CaGdAlO4 under high-power diode pumping," Opt. Lett. **32**(14), 1962–1964 (2007).
28. A. Klenner, M. Golling, and U. Keller, "High peak power gigahertz Yb:CALGO laser," Opt. Express **22**(10), 11884–11891 (2014).
29. A. Klenner, S. Schilt, T. Südmeyer, and U. Keller, "Gigahertz frequency comb from a diode-pumped solid-state laser," Opt. Express **22**(25), 31008–31019 (2014).
30. C. Hönninger, R. Paschotta, F. Morier-Genoud, M. Moser, and U. Keller, "Q-switching stability limits of continuous-wave passive mode locking," J. Opt. Soc. Am. B **16**(1), 46–56 (1999).

#233415 - $15.00 USD Received 30 Jan 2015; revised 17 Mar 2015; accepted 18 Mar 2015; published 25 Mar 2015

31. R. Paschotta, L. Krainer, S. Lecomte, G. J. Spühler, S. C. Zeller, A. Aschwanden, D. Lorenser, H. J. Unold, K. J. Weingarten, and U. Keller, "Picosecond pulse sources with multi-GHz repetition rates and high output power," New J. Phys. **6**, 174 (2004).
32. R. Grange, M. Haiml, R. Paschotta, G. J. Spuhler, L. Krainer, M. Golling, O. Ostinelli, and U. Keller, "New regime of inverse saturable absorption for self-stabilizing passively mode-locked lasers," Appl. Phys. B **80**, 151–158 (2005).
33. J. Peng, J. Miao, Y. Wang, B. Wang, H. Tan, L. Qian, and X. Ma, "Passive stabilization of a passively mode-locked Nd:GdVO4 laser by inverse saturable absorption," Opt. Commun. **281**(1), 141–145 (2008).
34. C. R. Phillips, A. S. Mayer, A. Klenner, and U. Keller, "SESAM modelocked Yb:CaGdAlO4 laser in the soliton modelocking regime with positive intracavity dispersion," Opt. Express **22**(5), 6060–6077 (2014).
35. C. Fiebig, G. Blume, C. Kaspari, D. Feise, J. Fricke, M. Matalla, W. John, H. Wenzel, K. Paschke, and G. Erbert, "12W high-brightness single-frequency DBR tapered diode laser," Electron. Lett. **44**(21), 1253–1255 (2008).
36. A. K. Chin and R. K. Bertaska, "Catastrophic Optical Damage in High-Power, Broad-Area Laser Diodes," in *Materials and Reliability Handbook for Semiconductor Optical and Electron Devices*, O. Ueda, and S. J. Pearton, eds. (Springer, 2013), pp. 123–147.
37. F. X. Kärtner, I. D. Jung, and U. Keller, "Soliton mode-locking with saturable absorbers," IEEE J. Sel. Top. Quantum Electron. **2**(3), 540–556 (1996).
38. J. Petit, P. Goldner, and B. Viana, "Laser emission with low quantum defect in Yb: $CaGdAlO_4$," Opt. Lett. **30**(11), 1345–1347 (2005).
39. L. R. Brovelli, U. Keller, and T. H. Chiu, "Design and operation of antiresonant Fabry-Perot saturable semiconductor absorbers for mode-locked solid-state lasers," J. Opt. Soc. Am. B **12**(2), 311–322 (1995).
40. G. J. Spühler, K. J. Weingarten, R. Grange, L. Krainer, M. Haiml, V. Liverini, M. Golling, S. Schon, and U. Keller, "Semiconductor saturable absorber mirror structures with low saturation fluence," Appl. Phys. B **81**(1), 27–32 (2005).
41. D. J. H. C. Maas, B. Rudin, A.-R. Bellancourt, D. Iwaniuk, S. V. Marchese, T. Südmeyer, and U. Keller, "High precision optical characterization of semiconductor saturable absorber mirrors," Opt. Express **16**(10), 7571–7579 (2008).
42. C. J. Saraceno, F. Emaury, C. Schriber, A. Diebold, M. Hoffmann, M. Golling, T. Südmeyer, and U. Keller, "Toward millijoule-level high-power ultrafast thin-disk oscillators," IEEE J. Sel. Top. Quantum Electron. **1**, 1100318 (2015).
43. C. J. Saraceno, C. Schriber, M. Mangold, M. Hoffmann, O. H. Heckl, C. R. E. Baer, M. Golling, T. Südmeyer, and U. Keller, "SESAMs for high-power oscillators: design guidelines and damage thresholds," IEEE J. Sel. Top. Quantum Electron. **18**(1), 29–41 (2012).
44. U. Keller and A. C. Tropper, "Passively modelocked surface-emitting semiconductor lasers," Phys. Rep. **429**(2), 67–120 (2006).
45. S. Chenais, F. Balembois, F. Druon, G. Lucas-Leclin, and P. Georges, "Thermal lensing in diode-pumped ytterbium lasers - part I: theoretical analysis and wavefront measurements," IEEE J. Quantum Electron. **40**(9), 1217–1234 (2004).
46. A. Yariv and P. Yeh, "The application of Gaussian beam. formalism to optical propagation in nonlinear media," Opt. Commun. **27**(2), 295–298 (1978).
47. A. A. Said, D. J. Hagan, M. J. Soileau, and E. W. V. Stryland, "Nonlinear refraction and optical limiting in 'thick' media," Opt. Eng. **30**, 1228–1235 (1991).
48. V. Magni, G. Cerullo, and S. De Silvestri, "ABCD matrix analysis of propagation of gaussian beams through Kerr media," Opt. Commun. **96**(4-6), 348–355 (1993).
49. S. Yefet and A. Pe'er, "A review of cavity design for Kerr lens mode-locked solid-state lasers," Appl. Sci. **3**(4), 694–724 (2013).
50. M. Haiml, R. Grange, and U. Keller, "Optical characterization of semiconductor saturable absorbers," Appl. Phys. B **79**(3), 331–339 (2004).
51. J. M. Dudley, G. Genty, and S. Coen, "Supercontinuum generation in photonic crystal fiber," Rev. Mod. Phys. **78**(4), 1135–1184 (2006).

1. Introduction

The SESAM (SEmiconductor Saturable Absorber Mirror) [1–3] has established itself as a key enabling technology for ultrafast lasers, and most if not all commercially available ultrafast lasers use the SESAM technology in industrial-compatible laser systems. SESAM modelocked diode-pumped solid state lasers (DPSSLs) have demonstrated quantum-noise limited performance [4] which benefits a large number of applications at gigahertz pulse repetition rates, such as high-speed optical communications [5–7], optical interconnects [8], optical clocks [9], lidar [10, 11], high-speed asynchronous optical sampling [12], analog-to-digital converters [13], and optical frequency metrology [14–16].

#233415 - $15.00 USD Received 30 Jan 2015; revised 17 Mar 2015; accepted 18 Mar 2015; published 25 Mar 2015

In the gigahertz pulse repetition rate regime fiber lasers suffer from low gain due to the short fiber length, limiting the pulse peak power to only a few dBm [17, 18]. Increasing the fiber length with harmonic modelocking (i.e. more than one pulse per cavity round-trip) introduces too much noise. The reduced peak power requires additional external amplification which increases the overall system complexity and noise performance. Ti:sapphire lasers reach up to 10-GHz pulse repetition rates and provide excellent performance for stabilized frequency combs [19]. At 5-GHz Ti:sapphire laser generated an average output power of 1.15 W with pulse durations as short as 24 fs [20]. Although ultrashort pulses are achieved with Kerr lens modelocking (KLM) [21], modelocking is not self-starting and the reduced pulse energy in a multi-GHz cavity limits the Kerr lens nonlinearity and therefore requires more critical cavity alignment. Moreover Ti:sapphire crystals require high-power green single-mode lasers for pumping which again increases complexity and cost.

Recent progress in gigahertz DPSSLs based on Yb-doped gain materials provide similar performance compared to Ti:sapphire lasers but SESAM modelocking provides self-starting and requires no critical cavity alignment. Based on KLM Yb-doped DPSSLs with the following pulse durations have been achieved: with Yb:KYW 146 fs with 15 mW of output power at a pulse repetition rate of 4.6 GHz [22] and with a ceramic Yb:Lu_2O_3 148 fs with 10 mW of output power at a pulse repetition rate of 6 GHz [23]. Much higher average power can be obtained with SESAM modelocking: with Yb:KGW 396 fs with 1.9 W average output power at a pulse repetition rate of 4.8 GHz [24], with Yb:CALGO [25–27] 47 fs in the megahertz pulse repetition rate regime [26] and 62 fs in a thin disk laser geometry [25]. Most recently we achieved record performance with SESAM modelocked Yb:CALGO lasers generating 60-fs pulses with 3 W of average output power at a pulse repetition rate of 1.8 GHz [28]. The peak power at 1 GHz was sufficient to demonstrate frequency comb offset stabilization without any further external pulse amplification and/or compression [29].

The challenge in SESAM modelocked Yb-doped DPSSLs for higher gigahertz pulse repetition rates is the increased tendency for Q-switching instabilities [30, 31]. Passive stabilization against Q-switched modelocking (QML) can be achieved with inverse saturable absorption using the absorber rollover [32] or an additional intracavity second-harmonic generation (SHG) process [33, 34]. The critical pulse energy for stable cw modelocking is lowered when the SESAM provides an additional inverse saturable absorption [32]. In 2005 Grange et al. derived a simple expression for the critical pulse energy (E_{crit}) for cw modelocking

$$E_{crit}^2 = \frac{F_{sat,abs}\, A_{abs}\, \Delta R}{\dfrac{1}{F_{sat,gain}\, A_{gain}} + \dfrac{1}{F_2\, A_{abs}}}. \qquad (1)$$

Thus stable modelocking can be achieved with an intracavity pulse energy larger than E_{crit} (Eq. (1)). $F_{sat,gain}$ and $F_{sat,abs}$ is the saturation fluence of the gain and of the absorber. F_2 is the inverse saturation fluence for induced absorption. A_{gain} and A_{abs} is the effective mode size in the gain and absorber. ΔR is the modulation depth of the absorber.

For a small mode size in the gain and the absorber the condition for stable cw modelocking (Eq. (1)) can be achieved even at the lower pulse energy typically obtained at gigahertz pulse repetition rates. Thus high-brightness pumping is required and for power scaling we need several high-brightness pumps or more complex diffraction-limited single-mode tapered diode-lasers [35], which suffer from low reliability and high sensitivity to optical feedback [36]. However, ultimately the damage induced by the small mode sizes in gain and absorber will ultimately limit the power scaling.

Here we provide a solution for further power scaling in the gigahertz pulse repetition rate regime using both low-brightness industrial-grade high-power pump laser diodes and larger

#233415 - $15.00 USD Received 30 Jan 2015; revised 17 Mar 2015; accepted 18 Mar 2015; published 25 Mar 2015

mode sizes in gain and absorber, addressing both limitations at the same time. We propose and demonstrate a passive stabilization mechanism, an all-optical Q-switching limiter, that suppresses QML in SESAM modelocked lasers using an intracavity Kerr lens. This Q-switching limiter damps fluctuations with higher peak power and therefore prevents possible damage due to Q-switched instabilities. In contrast to KLM no operation close to the cavity stability regime is required. We implement this Q-switching limiter in a SESAM modelocked Yb:CALGO DPSSL generating pulses as short as 96 fs with an average power of 4.1 W at a record-high pulse repetition rate of 5 GHz. The Q-switching limiter allowed for this power scaling at higher pulse repetition rates by increasing the cavity mode sizes and using high-power pumping with a commercial low-brightness laser diode array. The record-high pulse energy of 0.8 nJ and peak power of 7.5 kW at a pulse repetition rate of 5 GHz could previously only be achieved with Ti:sapphire laser oscillators [20] (see Fig. 1).

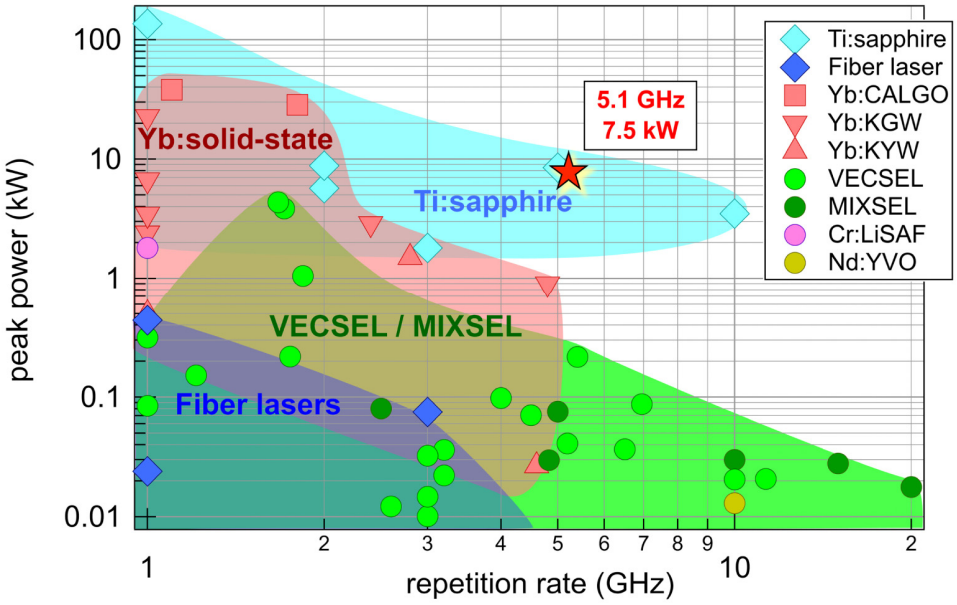

Fig. 1. Overview of gigahertz ultrafast laser oscillators without pulse compression and/or amplification: The peak power as a function of pulse repetition rate is shown for Ti:sapphire lasers, diode-pumped solid-state lasers, fiber lasers and modelocked semiconductor disk lasers (VECSELs and MIXSELs). The 5-GHz diode-pumped Yb:CALGO laser, presented in this paper (red star), stands out in particular for the record-high peak power which outperforms other diode-pumped oscillators and reaches the performance of Ti:sapphire lasers.

This paper is organized as follows. In the first section after this introduction the 5-GHz cavity setup is presented and the laser components are described in detail. This section is followed by a numerical analysis of the Kerr lens induced Q-switching limiter. Based on a 5-GHz laser cavity design, we used the measured SESAM parameters and the soliton modelocking theory [37] to investigate the effects of the limiter on Q-switching instabilities and the absorber operation. In last section we present the modelocking result based on a 5-GHz diode-pumped Yb:CALGO laser using this novel Q-switching limiter. This compact laser provides state-of-the-art performance with high power sub-100-fs pulses using a simple and robust cavity design in combination with straightforward SESAM modelocking and standard diode pumping.

#233415 - $15.00 USD Received 30 Jan 2015; revised 17 Mar 2015; accepted 18 Mar 2015; published 25 Mar 2015

2. SESAM modelocked diode-pumped Yb:CALGO laser

The cavity setup of the 5-GHz diode-pumped solid-state laser is shown in Fig. 2. The gain medium is an Yb(5% at.)-doped $CaGdAlO_4$ crystal (Yb:CALGO, a-cut) of 2-mm length. Broadband anti-reflection (AR) coatings on both facets enabled the operation under normal incidence. Yb:CALGO provides a broad and flat gain cross-section, which makes it ideally suited for the generation of ultrashort pulses below 100 fs [25, 28, 38]. The low quantum defect of 0.089 eV and the high thermal conductivity are very beneficial. However, compared to the more widely used Yb-doped tungstates (e.g. KYW, KGW) the higher gain saturation fluence of Yb:CALGO increases the tendency for QML [30]. To overcome this problem we implemented a Q-switching limiter into the laser design which strongly reduces these instabilities as described in more details in section 3.

The laser is pumped using a standard spatially multi-mode fiber-coupled diode laser (OCLARO, BMU25A-975-01-R03) with a maximum output power of 24 W at a wavelength of around 979 nm and an M^2 of 16. To keep the thermal load of the cavity low a polarizing beam splitter (PBS) removes the pump light which is polarized parallel to the a-axis of the Yb:CALGO crystal and which is only weakly absorbed. Two achromatic lenses and the PBS form a very simple, robust and powerful pumping configuration.

In multi-GHz laser oscillators the space for additional cavity elements is very limited. We therefore used a dispersive dichroic output coupler with an output coupling rate of 2.6%, negative group delay dispersion (GDD) of -600 fs^2 per pass and a radius of curvature (ROC) of 15 mm. The transmission window of the mirror at around 980 nm is used for pumping the Yb:CALGO crystal. A compact V-shaped cavity is formed by the output coupler, a curved high reflector (HR, 30-mm ROC) and the SESAM cavity end mirror (Fig. 2).

The SESAM is an antiresonant design [39, 40] with a single InGaAs quantum well absorber. A precise SESAM characterization was performed at a wavelength of 1051 nm with 95-fs pulses with a setup explained in [41]. The absorber provides a modulation depth of 1.4% with low nonsaturable losses of only 0.3% and a saturation fluence of 11.3 $\mu J/cm^2$. The SESAM was soldered on a copper heat sink and kept at room temperature using a Peltier element.

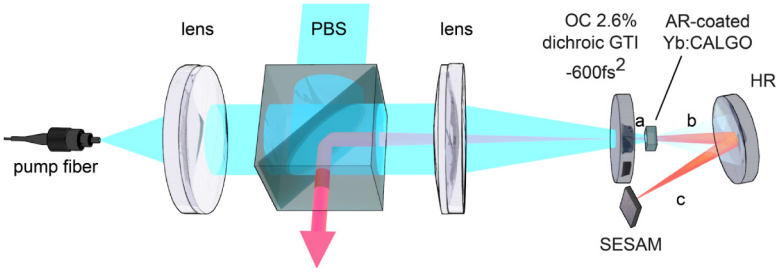

Fig. 2. SESAM modelocked Yb:CALGO laser stabilized by the Q-switching limiter: Experimental setup for a 5-GHz pulse repetition rate using a 2-mm long Yb:CALGO gain crystal. The pump light is polarized by a polarizing beam splitter (PBS). The gain crystal is end-pumped through a dichroic dispersive output coupler. This mirror has a radius of curvature (ROC) of 15 mm provides -600 fs^2 of GDD and an output coupling rate of 2.6%. The V-shaped cavity is defined by the output coupler end-mirror, a curved high reflector (HR) with an ROC of 30 mm and the SESAM end-mirror. The modelocked laser output is polarized perpendicular to the pump light and is reflected by the PBS in the opposite direction from the residual pump light. The intra- and extra-cavity beams are illustrated in red and the pump laser beam in blue.

3. Q-switching limiter: principle of operation and numerical analysis

Q-switching instabilities can be a severe problem for passively modelocked DPSSLs. During Q-switching the intracavity peak power can strongly exceed the values of stable cw

#233415 - $15.00 USD Received 30 Jan 2015; revised 17 Mar 2015; accepted 18 Mar 2015; published 25 Mar 2015

modelocking which can result in damage. Especially critical are dispersive mirrors which typically exhibit field enhancements to obtain negative dispersion [42]. SESAMs can be designed for higher damage threshold [43], however, the main damage mechanism is ultimately related to two-photon absorption (TPA) [43], but also Auger recombination and hot-carrier generation [43, 44].

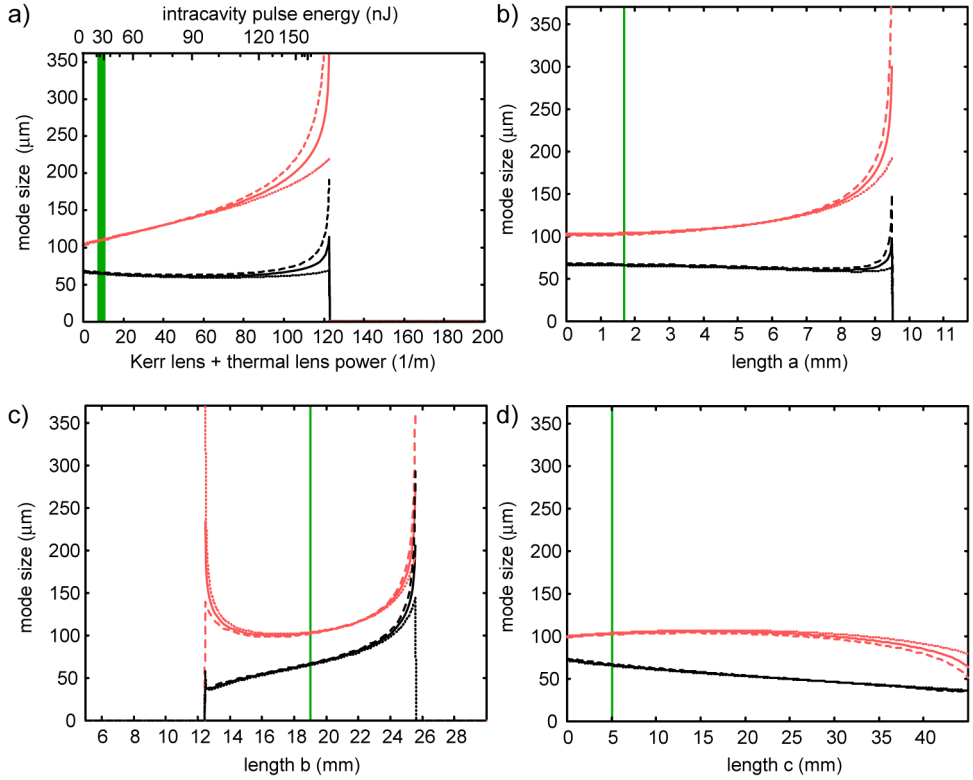

Fig. 3. Basic principles of Q-switching limiter and cavity stability ranges: Mode waist ($1/e^2$-mode radius) on SESAM (red) and gain crystal (black) in the 5-GHz cavity for the sagittal (dotted line), transversal (dashed line) and average mode size (solid-line) are shown. (a) shows the mode sizes as a function of the sum of Kerr lens and thermal lens focal power (lower x-axis) and the corresponding pulse energy (upper x-axis, see also Fig. 4(a)). The mode size on the SESAM is continuously increasing with the Kerr lens focal power $1/f_{Kerr}$, while the gain mode size is only changed by about 10% before the cavity approaches instability at about 120 diopters. During cw-modelocking the Kerr lens reaches values from 1.4 m^{-1} to 3.5 m^{-1}. We assume a thermal lens of about 10 m^{-1} based on simulations [45] (operation range indicated by the green rectangle). The mode size as a function of the position in the cavity for different Kerr lenses is visualized in Media 1. In (b), (c) and (d) the cavity stability ranges for the lengths a, b and c are shown. The cavity is operating well within the stability ranges. The green solid lines mark each length in the cavity (a = 1.7 mm, b = 19 mm and c = 5.1 mm).

3.1 Q-switching limiter: design calculations

For KLM a nonlinear focusing lens is induced by the Kerr effect (i.e. Kerr lens) to generate a fast saturable absorber which has lower loss for higher intensities and therefore favors pulse shortening. For the Q-switching limiter we use a Kerr lens in combination with a proper cavity design to achieve the opposite effect. In the latter case the Kerr lens results in beam defocussing and therefore a mode size increase on the intracavity optical elements. This reduces the peak intensities and dampens the onset of Q-switching instabilities. In contrast to KLM no operation close to the cavity stability regime is required (Fig. 3). This passive all-

#233415 - $15.00 USD Received 30 Jan 2015; revised 17 Mar 2015; accepted 18 Mar 2015; published 25 Mar 2015

optical mechanism can avoid optical damage caused by QML in SESAM modelocked ion-doped solid-state lasers. For our experiments we chose a cavity design in which the SESAM mode size continuously increases with the Kerr lens focal power, while the gain mode size does not strongly vary (Fig. 3(a)). We calculated a thermal lens in the Yb:CALGO crystal of about 10 m^{-1} for a pump power 14 W, i.e. an average output power of about 4 W, based on [45]. However, our analysis of the Q-switching limiter revealed only a weak dependence on the thermal lens. Please note that no KLM is used for pulse generation in this case. Furthermore no critical cavity stability regime has to be applied because the laser operates well within the cavity stability regime and the gain mode size barely changes with the Kerr lens. We note that a similar cavity design was already used for a 1.8-GHz Yb:CALGO laser [28]. This laser offered stable cw modelocking without QML which was not fully understood at that time. Here we present a detailed analysis of the stabilization mechanism of the Q-switching limiter implemented in a higher 5-GHz pulse repetition rate Yb:CALGO laser where Q-switching instabilities become even more severe.

To simplify the calculation of the Kerr lens it is common to make reasonable approximations [46, 47]. The gain medium is the dominant source for the Kerr nonlinearity. Hence, the Kerr lens is caused by the refractive index change Δn of the gain medium. For our calculations we assume a pure $\chi^{(3)}$ nonlinearity from the Kerr medium. When the nonlinear medium is assumed to preserve the Gaussian beam shape only phase changes near the beam axis are considered and a parabolic approximation can be used. In this case the radial change of the refractive index is approximated by $\Delta n(r) \approx \Delta n(0)\ (1 - r^2/\omega^2)$. Where $\Delta n(0)$ is the on-axis index change, ω the local $1/e^2$-mode radius. The resulting Kerr lens can be regarded as a stack of thin spherical lenses where each is represented by an individual ABCD matrix in the calculations [48]. To simplify the calculations we use a common approximation [49] that the Kerr lens is a single thin lens because the thickness of the gain crystal (L = 2 mm) is smaller than the confocal parameter of the laser beam (≈12 mm) and the shortest expected Kerr lens focal length (≈9 mm, see Fig. 3 (a)). Hence, the Kerr lens focal length f_{Kerr} is expressed by the nonlinear refractive index n_2 of the gain medium with mode size $A_{\mathrm{gain}} = 1/2\ \pi\ \omega_{\mathrm{gain}}^2$ and the peak power P_{pk}

$$f_{\mathrm{Kerr}}^{-1} = \frac{\pi\, n_2\, L}{A_{\mathrm{gain}}^2} P_{\mathrm{pk}} \ . \tag{2}$$

In case of a soliton modelocked laser [37] the Kerr lens focal power can be rewritten as a function of pulse energy, because the peak power is directly linked to the pulse energy E_{p} and the full-width-half-maximum (FWHM) pulse duration τ_p by

$$P_{\mathrm{pk}} = 0.88 \frac{E_{\mathrm{p}}}{\tau_{\mathrm{p}}} \ . \tag{3}$$

The pulse duration of the soliton pulse can be expressed by the cavity group delay dispersion (*GDD*) and Kerr nonlinearity, since

$$\tau_{\mathrm{p}} = 1.76\, \lambda \frac{|GDD|\, A_{\mathrm{gain}}}{\tau\, n_2\, L} \frac{1}{E_{\mathrm{p}}} \ . \tag{4}$$

Here λ is the center wavelength of the pulse spectrum. By inserting the Eqs. (3) and (4) into Eq. (2) we obtain

$$f_{\mathrm{Kerr}}^{-1} = \frac{1}{2\, \lambda |GDD|\, A_{\mathrm{gain}}} \left(\frac{\pi\, n_2\, L}{A_{\mathrm{gain}}} E_{\mathrm{p}} \right)^2 \ . \tag{5}$$

#233415 - $15.00 USD Received 30 Jan 2015; revised 17 Mar 2015; accepted 18 Mar 2015; published 25 Mar 2015

The Kerr lens focal power is proportional to the square of the soliton pulse energy and inversely proportional to the gain mode area to the power of 3. Using the dependence of the cavity mode sizes on the Kerr lens according to our design (Fig. 3), we can numerically solve Eq. (5) for our specific 5-GHz cavity using an ABCD-matrix formalism. For the nonlinear refractive index of Yb:CALGO we use $n_2 = 8^x10^{-20}$ m^2/W [27]. The cavity GDD is determined by measurements of the individual components with a white light interferometer. The dichroic GTI provides –600 fs^2 per pass, the CALGO crystal + 430 fs^2 and the SESAM + 25 fs^2. The Kerr lens focal power and the effective absorber fluence as a function of soliton pulse energy is then shown in Figs. 4(a)-(b). Pulse energies of about 150 nJ lead to a Kerr lens strong enough to cause an unstable cavity. The increasing SESAM mode size with the Kerr lens focal power leads to a clamping of the fluence incident on the SESAM for pulse energies above 60 nJ (Fig. 4(b) blue, solid-line). Thus above 60 nJ an increase in pulse energy does not result in an increased fluence since the SESAM mode size scales accordingly.

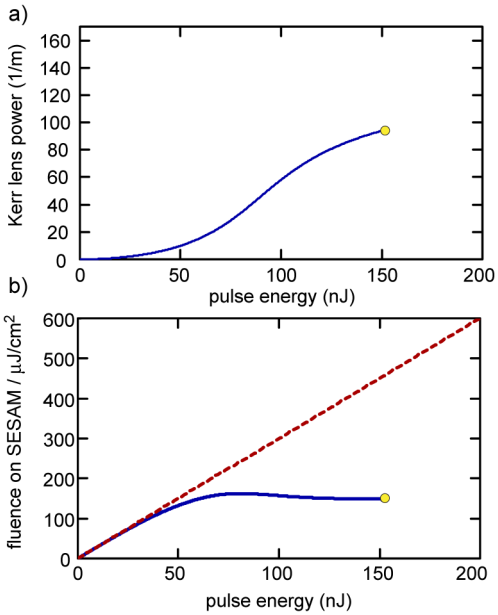

Fig. 4. Kerr lens focal power (a) and intracavity fluence on the SESAM (b) as a function of intracavity pulse energy. For pulse energies above 150 nJ the 5-GHz cavity becomes unstable (stability end is marked with yellow circle). The mode size change of the Kerr medium was taken into account. When the Kerr lens is disabled the fluence linearly increases with the pulse energy (red, dashed-line). With the Kerr lens at higher pulse energies the mode size on the SESAM is increased and therefore the fluence becomes clamped above 60 nJ. This already occurs well before the cavity stability limit. Thus no critical cavity alignment is required.

3.2 Q-switching limiter: SESAM reflectivity and induced saturable absorption

Clamping the fluence for high pulse energies strongly impacts the reflectivity curve of the saturable absorber. The model-function for the reflectivity R of a SESAM is given by [50]

$$R(F) = \left(1-\Delta R_{ns}\right)\frac{\ln\left(1+\dfrac{1-\Delta R_{ns}-\Delta R}{1-\Delta R_{ns}}\left(e^{F/F_{sat}}-1\right)\right)}{F/F_{sat}}e^{-F/F2}. \qquad (6)$$

#233415 - $15.00 USD Received 30 Jan 2015; revised 17 Mar 2015; accepted 18 Mar 2015; published 25 Mar 2015

with F, F_{sat} and F_2 as the pulse fluence, the saturation and inverse saturation fluence of the absorber, ΔR and ΔR_{ns} as the modulation depth and the nonsaturable losses respectively To obtain the SESAM reflectivity for the intracavity beam the spatial beam profile needs to be taken into account. The wings of the Gaussian beam saturate the absorber less than the beam center. The absorber reflectivity for a Gaussian beam is therefore [50]

$$R^{Gauss}(F) = \frac{1}{2F}\int_0^{2F} dzR(z) \ . \tag{7}$$

In Figs. 5(a)-(b) the SESAM reflectivity of a Gaussian beam is shown as a function of the intracavity pulse energy. The reflectivity increases with increasing pulse energy until a maximum reflectivity is reached. Higher fluences lead to a rollover of the reflectivity. This effect is referred to as inverse saturable absorption, quantitatively described by the inverse saturation fluence F_2 of the SESAM [32]. When we consider only TPA as a source for the inverse saturation, F_2 is proportional to the pulse duration and for soliton pulses inversely proportional to the pulse energy.

Without the Q-switching limiter the SESAM reflectivity strongly rolls over for high fluences, i.e. short pulse durations, and even decreases below the linear reflectivity (Figs. 5(a)-(b), red, dashed-line). This results in an increased absorbed fluence and thermal load in the SESAM. Especially critical are high pulse energies with short pulse durations during Q-switched modelocking. This behavior is investigated in Figs. 5(c)-(d). The absorbed energy and fluence, i.e. absorbed energy per area, are shown as a function of pulse duration for eight different pulse energies. Short pulses cause induced absorption and may result in optical damage of the saturable absorber.

With the Q-switching limiter all these effects are strongly suppressed. The passive all-optical limiter clamps the absorber fluence by defocussing the beam on the absorber (Media 1 and Figs. 5(a)-(b), blue, solid-line). As a result the rollover is damped and induced absorption is reduced. Therefore the reflectivity of the SESAM decreases much less at high fluences and the absorber operates well above the linear reflectivity until the cavity reaches instability with an increasing Kerr lens.

#233415 - $15.00 USD Received 30 Jan 2015; revised 17 Mar 2015; accepted 18 Mar 2015; published 25 Mar 2015

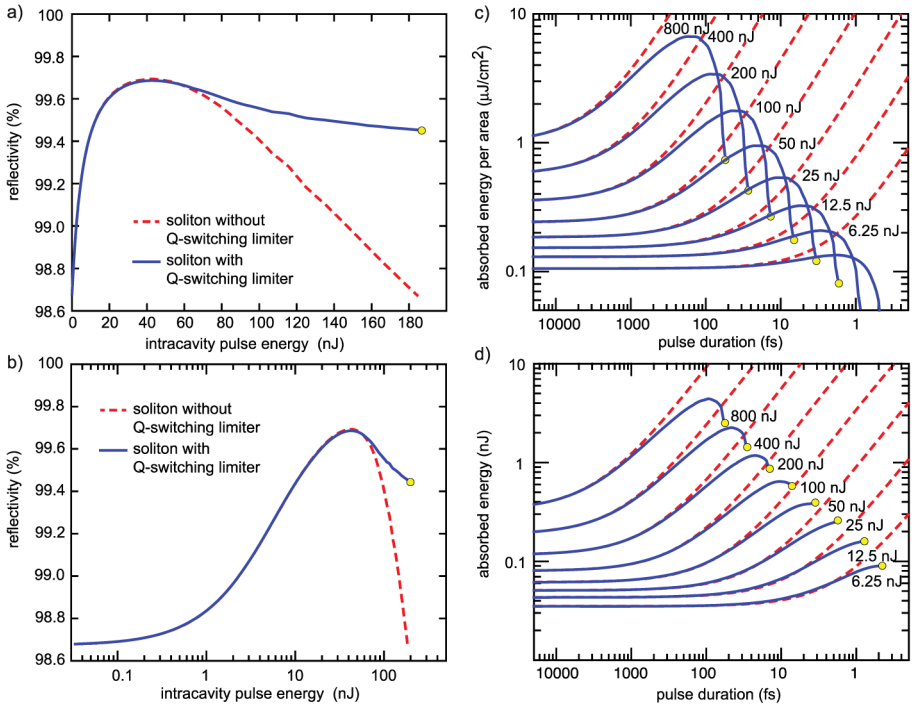

Fig. 5. (a), (b) SESAM reflectivity for a Gaussian beam profile as a function of intracavity pulse energy. For soliton pulses the pulse duration is directly mapped to the pulse energy (Eq. (4)). F_2 is assumed to be linearly dependent on the pulse duration. Without the Q-switching limiter the SESAM rollover is strong and the reflectivity drops below R_{lin} for high fluences (red, dashed line). For soliton pulses with a Q-switching limiter the SESAM rollover is reduced and the reflectivity is increased at high fluences. (c) Absorbed fluence and (d) absorbed energy by the SESAM for Gaussian beams as a function of pulse duration for different pulse energies: Without the Q-switching limiter the absorbed fluence strongly increases for short pulses possibly resulting in damage (red, dashed-line). With the Q-switching limiter the absorbed fluence is clamped to a maximum at short pulses. Shorter pulses lead to an unstable cavity configuration and hence a strong damping of Q-switched pulses (blue, solid-line). (Cavity stability end is marked with yellow circle; Scattering effects e.g. by surface defects are not included).

The moderate pulse energies during cw modelocking result in a weak Kerr lens, which has only a minor influence on the cavity stability. Below the cw modelocking threshold the laser operates in a regime where Q-switching instabilities can lead to the generation of high-energy pulses. Those pulse energies can exceed the cw modelocking values by orders of magnitude. With the Kerr lens induced limiter in place, the Q-switching instabilities are damped by the SESAM because the cavity mode size increases which distributes the absorbed energy over a larger area on the SESAM (Fig. 5(c)-(d) blue, solid-line). Thus Q-switching instabilities are effectively dampened and at the same time the absorbed fluence is limited to far below the damage threshold. Shorter Q-switched pulses induce a stronger Kerr lens which can even result in an unstable cavity configuration (Fig. 5(c)-(d) yellow circles). Furthermore at fluences below the SESAM rollover the Q-switching limiter does not affect the slope of the nonlinear reflectivity. Hence the reduced tendency for Q-switching instabilities by the inverse saturable absorption still provides some additional stabilization against Q-switching (Eq. (1)).

#233415 - $15.00 USD Received 30 Jan 2015; revised 17 Mar 2015; accepted 18 Mar 2015; published 25 Mar 2015

4. Modelocking results

The 5-GHz SESAM modelocked Yb:CALGO laser generates pulse durations as short as 95.5 fs. The pedestal-free second-harmonic autocorrelation trace fits well to a $sech^2$-pulse shape as expected from soliton modelocking (Fig. 6(a)). The measured optical spectrum is centered at 1054 nm with a full-width-half-maximum (FWHM) of 14.0 nm and fits well to a soliton spectral shape (Fig. 6(b)). The pulses are nearly transform-limited, the time-bandwidth product is 0.362 (1.13 x $sech^2$). We used a high-speed photo-diode to record the microwave spectrum of the laser. The signal of the repetition rate has a strong 80 dB signal to noise ratio (RBW = 10 kHz) without any sidepeaks (Figs. 6(c)-(d)). The clean microwave spectrum, the autocorrelation trace, the optical spectrum and the measured M^2 of the laser of <1.1 are typical for stable soliton modelocking. A high average output power of 4.1 W was obtained at a polarized pump power of 14.9 W (14.6 W incident on crystal), which corresponds to an optical-to-optical efficiency of 27.5% and a slope efficiency of 29.9% (Fig. 6(e)).

For a pump power below the modelocking threshold, we encountered self-pulsation of the laser, clearly visible by a flickering unstable SHG signal generated in an extracavity phase-matched lithium borate crystal. We note that without the Q-switching limiter in place damage of intracavity optics (GTI, crystal and SESAM) occurred at low pump powers below the modelocking threshold. Only with the Q-switching limiter in place we obtained stable cw modelocking. The laser output directly transferred into cw modelocking for pump powers above 10.8 W. No intermediate QML occurred, which can be explained by the Kerr lens induced all-optical Q-switching limiter. Stable cw modelocking was obtained with intracavity pulse energies from 23.5 nJ to 31.2 nJ. These energies fit with the effective SESAM rollover as shown in Figs. 5(a)-(b). For pump powers above 15 W fundamental modelocking stopped because of the SESAM rollover. Again we encountered self-pulsation of the laser but no QML. This unstable regime is usually a transition into double pulsing. However, the maximal available pump power was not sufficient to generate double-pulse modelocking.

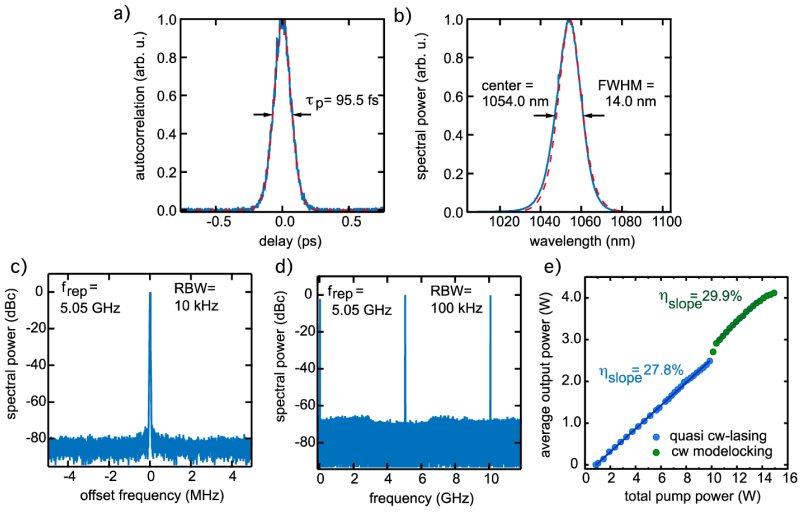

Fig. 6. SESAM modelocked 5-GHz Yb:CALGO laser: (a) second-harmonic autocorrelation trace with a pulse duration of 95.5 fs (blue: measurement, red dashed-line: $sech^2$-fit), (b) optical spectrum with a FWHM of 14.0 nm is centered at 1059.67 nm (blue: measurement, red dashed-line: soliton fit), (c) microwave spectrum for the 5-GHz pulse repetition rate with more than 60 dB SNR without sidepeaks for a resolution bandwidth (RBW) of 10 kHz, (d) microwave spectrum with a larger span and a RBW of 100 kHz and (e) laser average output power as a function of the pump power (measured after pump optics). A maximal output power of 4.1 W was achieved. RBW: resolution bandwidth of microwave spectrum analyzer.

#233415 - $15.00 USD Received 30 Jan 2015; revised 17 Mar 2015; accepted 18 Mar 2015; published 25 Mar 2015

5. Conclusion and outlook

We have introduced and demonstrated an all-optical Q-switching limiter to reduce Q-switching instabilities in SESAM modelocked diode-pumped Yb-doped solid-state lasers operating at gigahertz pulse repetition rates. The passive Q-switching limiter is based on a Kerr lens induced beam defocussing on the SESAM which clamps the pulse fluence on the SESAM for higher peak powers. No critical cavity alignment is required because this Q-switching limiter is fully functional well within the cavity stability regime. The Kerr lens also dampens the absorber rollover and therefore reduces SESAM damage. This results in a laser cavity which is stable for cw modelocking but unstable for Q-switched modelocking (QML). In addition, our numerical analysis shows that the SESAM nonlinear reflectivity at lower fluences is not affected by the Kerr lens and therefore the standard reduction of Q-switching tendencies by the rollover is still effective.

Using this passive all-optical Q-switching limiter we built the first diode-pumped laser that combines a high repetition rate of 5 GHz with high average power of 4.1 W and ultrashort pulses of 95.5 fs. This results in a record-high output pulse energy of 0.82 nJ and peak power of 7.5 kW directly from the 5-GHz Yb:CALGO laser oscillator. Such performance parameters could previously only be achieved from Ti:sapphire lasers or by additional external amplification and/or pulse compression.

This Q-switching limiter for SESAM modelocked diode-pumped solid state lasers (DPSSLs) is a key enabler for compact gigahertz frequency comb generation using standard high-power diode laser arrays for pumping. The demonstrated peak power even at 5 GHz pulse repetition rate will be sufficient to generate a coherent octave-spanning supercontinuum in a standard photonic crystal fiber for self-referencing a 5-GHz frequency comb [14, 51]. Our recent progress in stabilization of a 1-GHz diode-pumped solid-state laser frequency comb provides a better understanding of involved dynamics [29]. We will perform a full stabilization of the 5-GHz diode-pumped solid-state laser in the near future. Moreover, the Kerr lens induced all-optical Q-switching limiter opens the door for diode-pumped solid-state lasers with high peak power and repetition rates up to multiple-10 GHz pulse repetition rates. Thus such stabilized SESAM modelocked Yb-doped DPSSLs are expected to replace Ti:sapphire lasers for the next generation high-power gigahertz frequency combs.

Acknowledgments

This work was supported by the ETH Research Grant ETH-26 12-1 and the KTI project 17137.1 PFMN-NM.

#233415 - $15.00 USD Received 30 Jan 2015; revised 17 Mar 2015; accepted 18 Mar 2015; published 25 Mar 2015